

Vortex configurations of bosons in an optical lattice

Congjun Wu,¹ Han-dong Chen,² Jiang-ping Hu,³ and Shou-Cheng Zhang¹

¹*Department of Physics, McCullough Building, Stanford University, Stanford CA 94305-4045*

²*Department of Applied Physics, McCullough Building, Stanford University, Stanford CA 94305-4045*

³*Department of Physics and Astronomy, University of California, Los Angeles, CA 90095-1547*

The single vortex problem in a strongly correlated bosonic system is investigated self-consistently within the mean-field theory of the Bose-Hubbard model. Near the superfluid-Mott transition, the vortex core has a tendency toward the Mott-insulating phase, with the core particle density approaching the nearest commensurate value. If the nearest neighbor repulsion exists, the charge density wave order may develop locally in the core. The evolution of the vortex configuration from the strong to weak coupling regions is studied. This phenomenon can be observed in systems of rotating ultra-cold atoms in optical lattices and Josephson junction arrays.

PACS numbers: 03.75.Hh, 03.75.Lm, 05.30.Jp, 73.43.Nq

Vortices in charged or neutral superfluids (SF) can be created by applying an external magnetic field [1] or by rotating the system [2]. Properties of vortices are essential for understanding superfluidity [3]. Generally, vortices are topological defects in the SF order parameter with a 2π phase winding around the core. The SF order is suppressed near the core in an area characterized by the size of the healing length ξ . As a result, other orders competing with the SF order may develop there. In the context of high T_c superconductors, it was first proposed in the SO(5) theory that the vortex core is antiferromagnetic in underdoped samples[4]. This theoretical prediction has now been confirmed by numerous experiments[5]. Using the physics of the vortex core to study competing orders of doped Mott insulators is an important new direction in condensed matter physics[6].

Quantized vortices have been observed in rotating systems of dilute ultra-cold alkali atom gases [7, 8], drawing intense attentions both experimentally and theoretically [9, 10, 11, 12, 13, 14, 15, 16]. Most discussions up to now have been based on the Gross-Pitaevskii-Bogoliubov (G-P-B) equations, which assume that the particle density is given by the square of the amplitude of the SF order parameter. Thus, the minimum particle density is always located at the core, shown experimentally as a dark region in vortex imaging.

Near the SF-Mott insulator (MI) transitions, the G-P-B method ceases to work well. Theoretically, many investigations based on the Bose-Hubbard model are available now [17, 18] in the absence of rotation. The MI phases occur at the commensurate (integer) fillings when the hopping amplitude t is small compared with the Hubbard repulsion U . Transitions into the SF phase are triggered by either increasing t or changing the chemical potential. In the presence of the nearest neighbor repulsion W , the insulating CDW phases appear at half-integer fillings. However, the vortex configuration in this region has not been fully investigated. Experimentally, tremendous progress has been made in realizing the SF-MI transition in ultra-cold atomic systems in optical lattices [19, 20], as proposed in Ref. [21]. It would be interesting to further generate vortices in such systems.

Alternatively, Josephson junction arrays and granular superconductors in magnetic fields are also possible systems to study such vortices, where Cooper pairs behave like composite bosons.

In this article, we address the vortex configuration near the SF-MI and SF-CDW transitions. In the former case, the vortex core is close to the MI phase with a nearly commensurate filling while the SF dominates in the bulk area. In the latter case, the superfluid vortex with the CDW core behaves as a “meron” topological defect of the 3-vector pseudospin order parameter. These strong coupling configurations evolve to the weak coupling G-P-B vortex smoothly as t/U increases. Although the discussion below is for the rotating neutral bosonic system, it is also valid for the charged system in the magnetic field. Theoretical predictions obtained in this paper can be tested in these systems.

We study the 2D Bose-Hubbard model extended by a nearest neighbor repulsion W in the rotating frame

$$\begin{aligned} H = & -t \sum_{\langle \vec{r}_i, \vec{r}_j \rangle} \{ a^\dagger(\vec{r}_i) a(\vec{r}_j) e^{i \int_{\vec{r}_j}^{\vec{r}_i} d\vec{r} \cdot \vec{A}(\vec{r})} + h.c. \} \\ & + \sum_{\vec{r}_i} \{ V_{ex}(\vec{r}_i) - V_{cf}(\vec{r}_i) - \mu \} n(\vec{r}_i) \\ & + \frac{U}{2} \sum_i n(\vec{r}_i) (n(\vec{r}_i) - 1) + W \sum_{\langle \vec{r}_i, \vec{r}_j \rangle} n(\vec{r}_i) n(\vec{r}_j), \\ \vec{A}(\vec{r}) = & \frac{m}{\hbar} \vec{\Omega} \times \vec{r}, \quad V_{cf}(\vec{r}_i) = -\frac{1}{2} m \Omega^2 r_i^2, \end{aligned} \quad (1)$$

with μ the chemical potential, m the boson mass, $\vec{\Omega} = \Omega \hat{z}$ the rotation angular velocity, the position \vec{r} related to the axis of rotation, the vector potential \vec{A} due to the Coriolis force, V_{cf} the centrifugal potential, and V_{ex} the trapping potential. U is scaled to 1. For the charged bosonic system in the magnetic field \vec{B} , $\vec{A} = (e^*/2\hbar c) \vec{B} \times \vec{r}$ instead and the V_{cf} term is absent.

This model can be solved self-consistently by the mean-field (MF) approximation [17, 21], by decoupling the inter-site terms as

$$a^\dagger(\vec{r}_i) a(\vec{r}_j) \approx a^\dagger(\vec{r}_i) \langle a(\vec{r}_j) \rangle + (i \leftrightarrow j) - \langle a^\dagger(\vec{r}_i) \rangle \langle a(\vec{r}_j) \rangle,$$

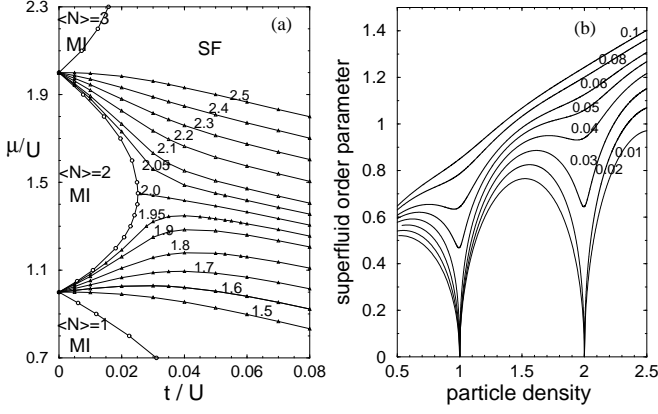


FIG. 1: (a) The ground state phase diagram for Bose-Hubbard model at $W = 0$ and $\Omega = 0$. Lines of equal particle densities are plotted with $\langle N \rangle = 2.5 \sim 1.5$ from top to bottom. (b) The SF order parameter $\langle a \rangle$ versus $\langle N \rangle$ at different values of $t/U = 0.1 \sim 0.01$ from top to bottom.

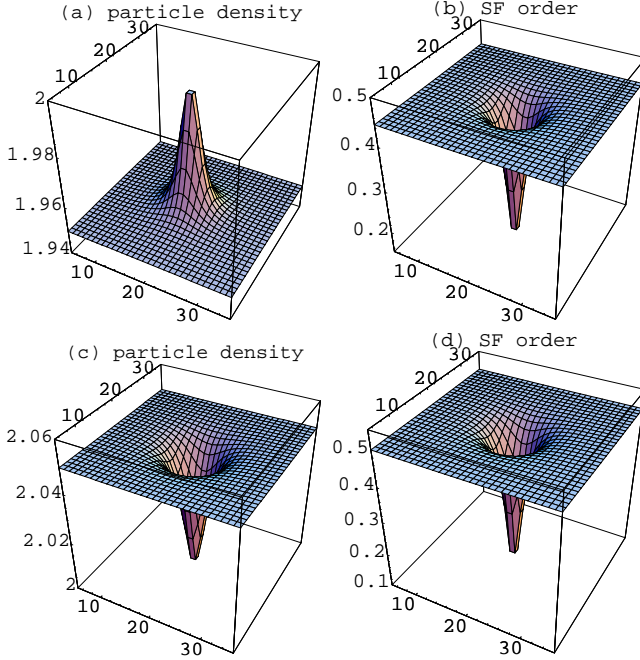


FIG. 2: Vortex configurations near the SF-MI phase boundary at $t/U = 0.02$ with bulk particle density $\langle N \rangle = 1.95$ (in (a) and (b)) and $\langle N \rangle = 2.05$ (in (c) and (d)). The left hand side (a) and (c) are the particle density distributions; the right hand side (b) and (d) are the SF order distributions.

$$n(\vec{r}_i)n(\vec{r}_j) \approx n(\vec{r}_i)\langle n(\vec{r}_j) \rangle + (i \leftrightarrow j) - \langle n(\vec{r}_i) \rangle \langle n(\vec{r}_j) \rangle. \quad (2)$$

$\langle a(\vec{r}_j) \rangle$, $\langle n(\vec{r}_j) \rangle$ are expectation values on the MF ground state, which is approximated by a product wave function of the form $|\Psi\rangle_G = \prod_{\vec{r}_i} |\psi(\vec{r}_i)\rangle$. We cutoff each single-site Hilbert space up to 10 particles which is sufficient for experimental values $\langle N \rangle \approx 1 \sim 3$ [19]. The SF and CDW order parameters are defined as $\langle a(\vec{r}_i) \rangle$ and $(-)^{r_i}(\langle n(\vec{r}_i) \rangle - \langle N \rangle)$ respectively, where $\langle N \rangle$ is the

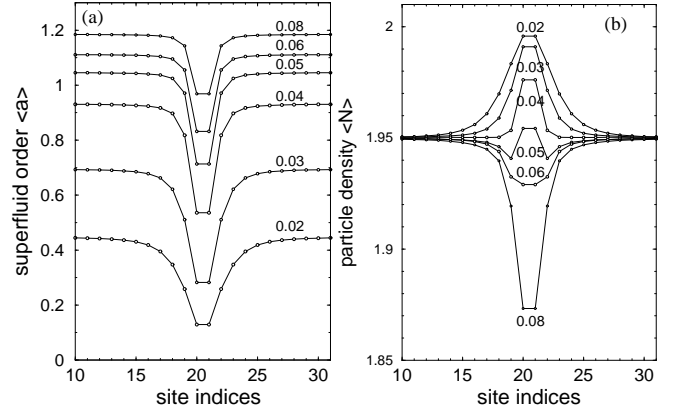


FIG. 3: The evolution of vortex configurations at $\langle N \rangle = 1.95$ as increasing t/U . SF amplitudes in (a) and particle densities in (b) are shown along a path cut from (10,20) to (30,20) in the 40×40 system. $t/U = 0.02 \sim 0.08$ from bottom to top in (a) and top to bottom in (b).

bulk average particle density. This simple MF theory describes the SF-MI transitions and extrapolates well into the intermediate coupling region [17, 18]. For example, the relation of the SF order $\langle a \rangle$ v.s. t/U from the MF theory is in good agreement with that of the Monte-Carlo simulations at both commensurate (integer) and incommensurate fillings[22].

Before discussing the vortex problem, it is helpful to recall the well-known phase diagram when $\Omega = 0$ [17] (Fig. 1 (a)). From the equal density contours we can see an approximate particle-hole (p-h) symmetry with respect to $\langle N \rangle = 2$ near the phase boundary: μ drops or increases with increasing t/U when $\langle N \rangle \geq 2$ or < 2 respectively. These can be viewed as particle or hole SF, but this difference no longer exists as t/U becomes large, where μ drops with increasing t/U for both cases, i.e., the system evolves from the strong to weak coupling region. In Fig. 1 (b), SF order v.s. $\langle N \rangle$ is shown at different values of t/U . The SF order parameter increases monotonically with $\langle N \rangle$ at large t/U , while the commensurate filling suppresses the SF order prominently at small t/U , eventually leading to the MI phase. At $t/U \approx 0.08$, the suppression disappears even at $\langle N \rangle = 1$, which marks the cross-over into the weak coupling region.

We study the single vortex problem in a $40a_0 \times 40a_0$ (a_0 being the lattice constant) system around which the circulation of \vec{A} is 2π and thus $\Omega = \hbar/(2mL^2)(L = 40a_0)$ correspondingly. The rotation center is located at the center of the central plaquette. We further simplify the problem by dropping the V_{ex} and V_{cf} terms, since they behave smoothly near the center of the trap and they can cancel each other if the Ω is close to the trap frequency.

Two typical vortex configurations near the SF-MI transition are shown in Fig. 2 (a) ~ (d) with $t/U = 0.02$, where the particle densities in cores are maximal or minimal respectively. The vortex core is located at the center of the plaquette with the reduced SF order on the sites

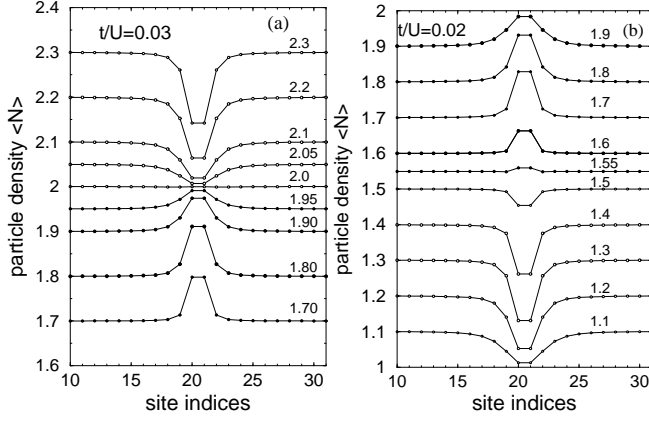


FIG. 4: The evolution of vortex particle density distribution at fixed $t/U = 0.03$ (a) and 0.02 (b) with varying bulk values $\langle N \rangle$ along the same path in Fig. 3. (a) From top to bottom, $\langle N \rangle = 2.3 \sim 1.7$. (b) From top to bottom, $\langle N \rangle = 1.9 \sim 1.1$.

nearby. Roughly speaking, the square of the superfluid amplitude, $|\langle a \rangle|^2$, is proportional to $|\langle N \rangle - N_0|$ near the transition, where $N_0 = 2$ here is the nearest commensurate value. The local particle density in the core should be closer to the commensurate value in order to suppress the SF order. As a result, the particle density reaches a maximum or minimum when the bulk density $\langle N \rangle$ is slightly smaller or larger than the commensurate value. The former case can also be understood as the vortex of the hole superfluid, where the hole density goes to a minimum at the core. This contrasts with the case of fermionic superfluidity, where the Cooper pairs are broken into normal particles in the core with total particle density almost unchanged, and also with the case of the weak coupling bosonic system where the only possibility is the depletion of the core particle density. As we approach the vortex core from outside, the hopping process is frustrated and thus effectively t/U becomes small because of the phase winding of the SF order. As a result, the vortex core is driven closer to the MI state than the bulk area. We also check the vortex configuration with integer value of $\langle N \rangle = 2$ at the same value of t/U , where the particle density distribution is uniform with suppressed SF order in the core.

We further discuss the evolution of the vortex core configuration from the strong to the weak coupling regions. The bulk particle density is fixed at $\langle N \rangle = 1.95$ with increasing t/U as shown in Fig. 3. The SF order increases and the healing length ξ decreases away from the SF-MI boundary along this direction of evolution. On the other hand, the weak coupling expression $\xi/a_0 = \sqrt{t/(U\langle N \rangle)}$ states that ξ increases with increasing t/U . Thus we can infer that ξ 's minimum value appears in the intermediate coupling region. The vortex core with extra particle density survives until $t/U \approx 0.05 \sim 0.06$, after which it crosses over gradually to that with depleted particle density at large t/U . This transition agrees with the be-

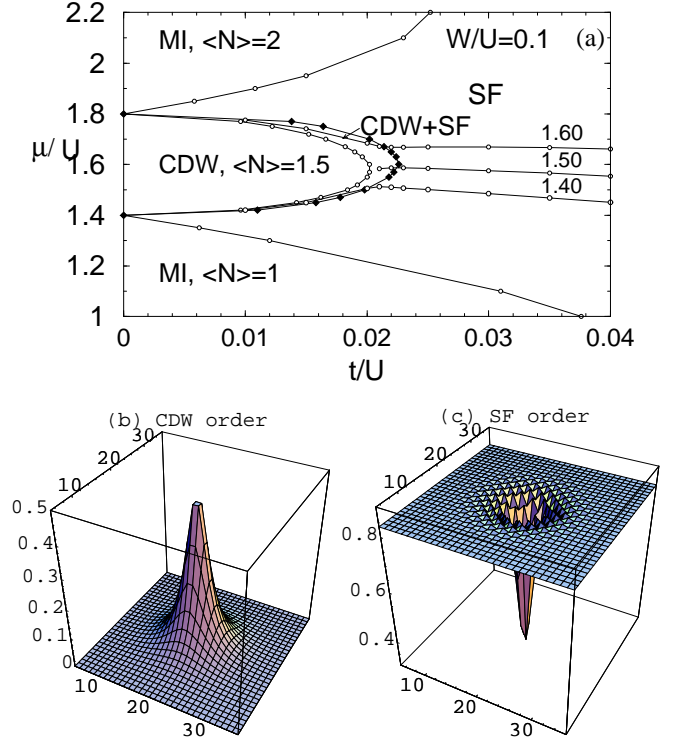


FIG. 5: (a) Phase diagram of the extended Bose-Hubbard model with $W/U = 0.1$ around $\langle N \rangle = 1.5$. Lines of equal particle densities are plotted with $\langle N \rangle = 1.6 \sim 1.4$ from top to bottom. The CDW (b) and SF (c) order distributions in the vortex configuration near the CDW phase with $t/U = 0.023$ and bulk average $\langle N \rangle = 1.5$.

havior of the SF order *vs.* $\langle N \rangle$ when the system is not in rotation. In that case, at the same filling level, we check that the suppression due to the commensurate filling also vanishes around a similar value of t/U . When t/U is larger than 0.06, the vortex configuration is already similar with the weak coupling case. We also check the above evolution with fixed $\langle N \rangle = 2.05$. The feature of SF order is similar with that in Fig. 3 (a), and the minimum particle density is always located in the core. When t/U is less than an intermediate value around 0.05, the core particle density is close to the commensurate value 2.0. When t/U grows larger, it drops further. This also agrees with the evolution picture from strong to weak coupling physics.

Another evolution from the particle-like vortex core to the hole-like core with fixed t/U in the strong coupling region and varying $\langle N \rangle$ is shown in Fig. 4 (a). We choose the region close to the MI phase with $\langle N \rangle = 2$, where the approximate p-h symmetry is valid, with t/U fixed at 0.03 and $\langle N \rangle$ varying from 2.3 to 1.7. As a result, the difference between the core particle density and the bulk value changes from negative to positive as the bulk density passes $\langle N \rangle = 2$. This point is the closest one to the tip of the MI phase along the evolution, where the minimum of the SF order and the maximum of ξ also

lie. In Fig. 4 (b), such evolution is shown along the path $t/U = 0.02$ connecting two neighboring MI phases with $\langle N \rangle = 2$ and 1. The core configuration is close to the MI phase with $\langle N \rangle = 2$ on the top, and becomes close to the MI phase with $\langle N \rangle = 1$ at the bottom. Around $\langle N \rangle = 1.55$, the density distribution becomes almost uniform. This point is the maximum of the SF order and the minimum of ξ because it is the farthest point from the MI, which is just opposite to Fig. 4 (a). In both Fig. 4(a) and (b), the tendencies to MI phase in the vortex core are strong when the average $\langle N \rangle$ is close to an integer, and becomes weaker as $\langle N \rangle$ away from commensurate fillings.

Next we turn on the nearest neighbor repulsion $W/U = 0.1$. In the absence of rotation, CDW phases appear between two neighboring commensurate MI phases at half-integer fillings when t/U is small [23]. At large values of t/U , SF phases stabilize as usual. Between the CDW and the SF phases, the mean field theory gives a small area of the coexistence of CDW and SF order, i.e., the supersolid phase [23]. These are shown in Fig. 5 (a) with the equal density lines around $\langle N \rangle = 1.5$. It is well known that the hard-core boson model can be mapped into spin 1/2 XXZ model in a magnetic field, and thus the CDW and SF orders can be unified in a 3-vector pseudospin picture. With the releasing of the hard core constraint, the above mapping is still approximately valid in the sense that the spin up and down states correspond to two nearest integer number states on each site. The vortex configuration at $t/U = 0.023$ with bulk particle density $\langle N \rangle = 1.5$ is shown in Fig. 5 (b) and (c). The SF order dominates outside the core, while the CDW order develops together with the suppression of the SF order in the core. In the pseudo-spin picture, this is a kind of topological defect called “meron”, where the pseudo-spin pointing along z axis at the origin gradually changes to lying in the x - y plane with a winding number 1 around the origin when far from it. This vortex configuration also evolves to the weak coupling one at large value of t/U with the disappearance of the CDW order in the core. This situation is similar to the behavior of the superspin in the $SO(5)$

theory of the antiferromagnetic vortex core[4, 5].

In previous experiments, the vortex core with size $2\xi \approx 0.4\mu\text{m}$ is too small to observe directly by optical methods. A time-of-flight expansion is needed before optical absorption imaging[8]. On the optical lattice, the vortex core is larger. The typical core size in our calculations is estimated at $5 \sim 6$ lattice constant a_0 ($a_0 = 0.426 \mu\text{m}$ in Ref. [19]), i.e. about $2 \mu\text{m}$. The resonant probe laser beam can be focused to this size at the level of current technology [24]. Thus without turning off the trap, it is possible to image the core particle density distribution non-destructively by scanning the probe laser beam. It would be interesting to find the anomalous vortex with the maximum particle density in the core. Another possible realization is the Josephson junction array. The non-uniform charge distributions in the vortex configuration result in electric fields [25]. Thus it is possible to determine the filling in the vortex core with respect to the outside by measuring electric field distributions.

In summary, we have studied vortex structures of the strong coupling boson systems. Near the SF-MI transition, the vortex core is more strongly coupled compared to the bulk area and is thus closer to the MI phase with suppressed SF order. The particle density in the core can be either the maximum or the minimum of the whole system, always approaching the nearest commensurate density of the Mott insulator. Near the SF-CDW transition, a superfluid meron-like vortex is found with a CDW core. All of these strong coupling vortex configurations evolve to the conventional weak coupling one as t/U increases.

We thank G. Baym, M. Beasley, B. A. Bernevig, I. Bloch, C. Chin, S. Chu, A. L. Fetter, N. Gemelke, P. SanGiorgio, E. Mukamel, and F. Zhou for helpful discussions. This work is supported by the NSF under grant numbers DMR-9814289, and the US Department of Energy, Office of Basic Energy Sciences under contract DE-AC03-76SF00515. CW and HDC are also supported by the Stanford Graduate Fellowship program.

-
- [1] A. A. Abrikosov, Soviet Phys. JETP, **5** 1174(1957).
 - [2] E. M. Lifshitz and L. P. Pitaevskii, *Statistical Physics* part 2, 3rd edn(Oxford:Pergamon) (1980).
 - [3] H. Kleinert, Gauge fields in condensed matter, Vol I World Scientific, Singapore (1989); H. Kleinert, Lett. Nuovo Cimento **35**, 405 (1982).
 - [4] S.C.Zhang, Science, **275**, 1089 (1997); D. Arovas *et al*, Phys. Rev. Lett.**79**, 2871(1997),
 - [5] B. G. Levi, Physics Today, **55** (2), 14-16 (2002).
 - [6] S. Sachdev, S.C. Zhang, Science **295**, 452 (2002).
 - [7] M. R. Matthews *et al*, Phys. Rev. Lett. **83**, 2498(1999).
 - [8] K. W. Madison *et al*, Phys. Rev. Lett. **84**, 806(2000).
 - [9] B. P. Anderson *et al*, Phys. Rev. Lett. **85**, 2857 (2000).
 - [10] K. W. Madison *et al*, J. Mod. Opt. **47**, 2715(2000).
 - [11] F. Chevy *et al*, Phys. Rev. Lett. **85**, 2223(2000).
 - [12] J. E. Williams *et al* Nature **401**, 568 - 572 (1999).
 - [13] A. L. Fetter *et al*, J. Phys. : Condens. Matter **13**, R135-R194 (2001).
 - [14] G. Baym *et al*, Phys. Rev. Lett. **76**, 6 (1996).
 - [15] D. A. Buttset *et al*, Nature, **397**, 327(1999).
 - [16] U. R. Fischer and G. Baym, Phys. Rev. Lett. **90**, 140402 (2003).
 - [17] M. P. A. Fisher *et al* Phys. Rev. B **40**, 546 (1989).
 - [18] K. Sheshadri *et al*, Europhys. Lett. **26**, 545(1993).
 - [19] M. Greiner, *et al*, Nature **415**, 39(2002).
 - [20] C. Orzel, *et al*, Science **291**, 2386(2001).
 - [21] D. Jaksch, C. Bruder, J. I. Cirac, C. W. Gardiner, and P. Zoller, Phys. Rev. Lett.**81**, 3108(1998).
 - [22] W. Krauth *et al*, Phys. Rev. Lett. **67**, 2307(1991).
 - [23] C. Pich *et al*, Phys. Rev. B **57**, 13712(1998).
 - [24] S. Chu, private communication.
 - [25] M. Beasley, private communication.